LAPPEENRANTA UNIVERSITY OF TECHNOLOGY

LUT School of Engineering Science

Degree program of Chemical Engineering

Petro Silvonen

CATALYTIC UPGRADING OF FATTY ACIDS TO HYDROCARBONS IN SEMI-BATCH REACTOR AND STUDY OF THE PRODUCT PROPERTIES

Examiners: Prof. Tuomo Sainio
M.Sc Jukka Myllyoja

Instructor: M.Sc Jukka Myllyoja

FOREWORDS

This thesis was completed in Neste Oyj R&D Technology Centre in Porvoo during 8/2017 – 1/2018.

I thank for the guidance and support received from project group at Neste, Tuomo Sainio at LUT and especially my instructor Jukka Myllyoja for suggesting this interesting thesis proposal in the first place. I am very happy of the opportunity to work with multiple greatly helpful and motivational people. Special thanks also to Kaija Isokoski, Rami Piilola, Sebastian Lahtinen and Sonja Kouva – Without you this thesis would not have been possible.

I would also like to thank my friends, classmates and family (Johanna, Mika, Timka and Tilma) who supported me during my studies. The past six years have been the greatest time of my life so far and I am highly anticipating the future challenges in chemical engineering field awaiting after graduation.

Porvoo, 1st of March 2018.

Petro Silvonen

TIIVISTELMÄ

Lappeenrannan teknillinen yliopisto
LUT School of Engineering Science
Kemiantekniikan koulutusohjelma

Petro Silvonen

Rasvahappojen katalyyttinen konvertointi hiilivedyiksi puolipanosreaktorissa ja lopputuoteominaisuuksien tarkastelu

Diplomityö

2018

45 sivua, 27 kuvaa, 21 taulukkoa ja 5 liitettä

Tarkastajat: Prof. Tuomo Sainio
DI Jukka Myllyoja

Hakusanat: rasvahappo, katalyytti, puolipanos, hiilivety

Perinteisten fossiilisten polttoaineiden ympäristöhaasteet ja hupenevat raaka-ainevarannot ovat ohjanneet maailmaa biopolttoaineiden tuotantoon viime vuosikymmenten aikana. Rasvat ja öljyt ovat raaka-aineina tärkeä osa biopolttoaineiden tuotantoa ja ne ovat myös mahdollistaneet uusiutuvien ja kestävien kemikaalien ja muiden biotuotteiden valmistuksen.

Tämän työn kirjallisessa osassa tarkastellaan erityisesti rasvahappojen prosessointia ketoneiksi ja kirjallisuudessa esiteltyjä mekanismeja.

Kokeellisessa osassa rasvahappojen reaktioreittiä hiilivedyiksi tutkittiin palmitiinihapon ja oleiinihapon avulla laboratoriomittakaavan puolipanosreaktorissa. Tarkastellut ketonointikokeet loivat myös pohjan laajemmalle Parr-mittakaavan reaktorikokeiden menetelmänkehitykselle. Työssä tutkittiin rasvahappojen lisäksi muiden syöttöaineiden sopivuutta ketonointiin.

Tulosten perusteella Parr-mittakaavan puolipanosreaktori on toimiva laitteisto rasvahappojen ketonointiin ja vedytykseen liittyvien tutkimustehtävien suorittamiseen, sillä erityisesti näytteenotto reaktorista mahdollistaa laajan datan keruun kokeista. Tulosten perusteella kaksoissidoksellisten rasvahappojen läsnäolo aiheuttaa raskaiden hiilivetyjen muodostumista biovahatuotteessa ainoastaan 3, 5, ja 7 % tasolla alkuperäisestä rasvahappokoostumuksesta riippuen. Lopputuotteiden viskositeetti-indeksit olivat välillä 112-116.

ABSTRACT

Lappeenranta University of Technology
LUT School of Engineering Science
Degree Program of Chemical Engineering

Petro Silvonen

Catalytic upgrading of fatty acids to hydrocarbons in semi-batch reactor and study of the product properties

Master's Thesis

2018

45 pages, 27 figures, 21 tables and 5 appendixes

Examiners: Prof. Tuomo Sainio
M.Sc Jukka Myllyoja

Keywords: fatty acid, catalyst, semi-batch, hydrocarbon

Environmental concerns of traditional fossil fuels and their decreasing feedstock reserves have driven world to production of biofuels during the past few decades. Critical part of biofuel production as feedstock have been fats are oils which also allow manufacturing of renewable and sustainable chemicals and other bio-products.

In the theoretical part of this study, processing of fatty acids especially to ketones was studied. Also, the main mechanisms found in the literature were discussed.

In the experimental section, catalytic upgrading of fatty acids to hydrocarbons was examined with palmitic acid and oleic acid in laboratory scale semi-batch reactor. The ketonization tests carried out also provided foundation for further test method development of Parr-scale reactor setup. Additionally, potential of other feedstock outside of the fatty acid pool for ketonization was studied.

Based on the experiments, Parr-scale semi-batch reactor is valid method for wide range of research tasks involving ketonization or hydrodeoxygenation of fatty acids. Wide range of data can be obtained with reactor sampling. Based on the results, heavy fraction in biowax product is 3, 5 and 7 % depending on the amount of double-bonded fatty acids in the initial feedstock. End products with viscosity index 112 to 116 were obtained from the experiments.

LIST OF ABBREVIATIONS AND SYMBOLS

FTIR	Fourier-Transform infrared spectroscopy
GC	Gas chromatography
GPC	Gas permeation chromatography
HDO	Hydrodeoxygenation
IR	Infrared spectroscopy
M	Metal/metal-ion
MS	Mass spectrometry

TABLE OF CONTENTS

1 INTRODUCTION 3
2 FATS, OILS AND FATTY ACIDS 4
2.1 Fats and oils and their processing 4
2.2 Main fatty acid reaction paths 6
2.2.1 Decarboxylation and decarbonylation 7
2.2.2 Hydrogenation 8
2.2.3 Deoxygenation 8
3 KETONIZATION 9
3.1 Ketonic decarboxylation 9
3.2 Further processing with hydrodeoxygenation 10
3.3 Ketonization mechanisms 10
3.3.1 Bulk and surface ketonization 10
3.3.2 Ketonization enabled by α-hydrogen 12
3.3.3 Ketene-based mechanism 12
3.3.4 β-keto acid mechanism 13
5 MATERIALS AND METHODS 14
5.1 Used materials 14
5.1.1 Feeds 14
5.1.2 HDO feedstock 15
5.1.3 Catalysts 15
5.2 Experimental equipment and test procedures 18
5.2.2 Herzog distillation 22
5.2.3 Gas chromatography analysis 22
5.2.4 Additional analyses 24
6 RESULTS AND DISCUSSION 25
6.1 Gas chromatography results' background 25
6.2 Thermal stability test for C16:0 27
6.3 Ketonization run parameters' testing 27
6.4 Effects of temperature and pressure 31
6.5 C16:0 and C18:1 ketonization tests 36

6.6 Other feedstock ketonization (FAME and FAEE) 38
6.7 Hydrodeoxygenation tests 39
8 CONCLUSIONS 43
REFERENCES 45
APPENDICES 48

1 INTRODUCTION

During the past few decades, environmental concerns and diminishing fossil fuel reserves have pushed mankind to discover renewable and sustainable resources for fuel and chemical production. Extensive research and development in the area have allowed invention and further optimization of vast scale of processes, catalysts and other related technical solutions.

Fats and oils have played a critical role in the production of biofuels and especially biodiesel for over 25 years. The feedstock has been derived from e.g. variety of vegetable oils, animal fats, recycled waste oils and even microbial oils. According to Mittelbach (2015) rape seed oil (Canola), soybean oil and palm oil are the major feedstock dominating the global biodiesel market and the world's biodiesel production is estimated to be 15-16 million tons per year.

In addition to fuels, fats and oils can be step-by-step processed into renewable chemicals and base oils. One of these processes is ketonization, which enables the removing of the highly reactive carboxylic functional groups while increasing the carbon chain length. The formed ketones are building blocks for further refining, eg. hydrodeoxygenation, to obtain suitable product for the required application. (Pham et al. 2016)

Main focus of the literature review of this thesis is covering the principles of fatty acid processing into hydrocarbons through ketonization and subsequent hydrodeoxygenation (HDO). In the experimental part, this two-step process, yielding a long-chain hydrocarbon product, is simulated through experiments with a laboratory scale semi-batch autoclave system. In ketonization, different factors affecting the reaction and product composition are studied and after HDO the final product samples, which are suitable for e.g. biowax production, are examined in terms of general chemical composition, heavies' formation, viscosity and other analyses.

2 FATS, OILS AND FATTY ACIDS

This chapter focuses on the principles of bio-oils and especially fatty acids. Also main fatty acid reaction paths are examined.

2.1 Fats and oils and their processing

Fats and oils are defined based on their physical state: in ambient temperature fats are solid and oils are liquid. Commercial fat and oil products can be derived from animal carcasses by rendering, pressing or through solvent extraction. These versatile materials are mainly consisting of triacylglycerols (Figure 1, esters of glycerol and fatty acids) and wax esters (esters of fatty acids) with long chain aliphatic alcohols, sterols, tocopherols or similar compounds. They can be derived from animal and vegetable sources which typically contain an even carbon number due to their original condensation path from two carbon units. However, branched or odd-numbered carbon number containing fatty acids can be found in small concentrations in for example natural triacylglycerols. Chain lengths of even carbon number chains range from 4 to 22. (Hasenhuettl 2016)

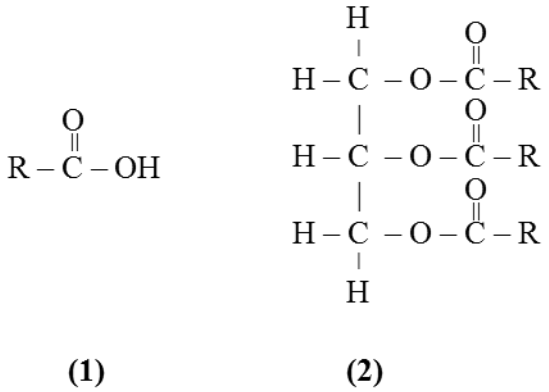

(1) **(2)**

Figure 1 General structure of (1) fatty acid and (2) triacylglycerol (Hasenhuettl 2016).

Fatty acids (Figure 1) are either saturated, monounsaturated or polyunsaturated based on the amount of double bonds in the chain. Double bonds that occur in fatty acids are

typically cis (Z) configurated. Common fatty acids found in triacylglycerols are shown in Table 1 where fatty acids are abbreviated with carbon number and the amount of double bonds. The most common fatty acids in vegetable and animal fats are lauric (12:0), palmitic (C16:0), stearic (C18:0), oleic (C18:1), linoleic (C18:2) and linolenic (C18:3) acids. Examples of common fatty acids are shown in Table I. (Srivastava & Prasad 2000)

Table I Examples of fatty acids found in naturally occurring triglycerides (Srivastava & Prasad 2000)

Fatty acid	**Structural formula**	**Abbreviation**	**Primary source**
Butyric	$C_4H_8O_2$	4:0	butter
Caproic	$C_6H_{12}O_2$	6:0	butter
Caprylic	$C_8H_{16}O_2$	8:0	coconut
Capric	$C_{10}H_{20}O_2$	10:0	coconut
Lauric	$C_{12}H_{24}O_2$	12:0	coconut, palm kernel
Myristic	$C_{14}H_{28}O_2$	14:0	coconut, palm kernel
Palmitic	$C_{16}H_{32}O_2$	16:0	palm, cottonseed, butter
Palmitoleic	$C_{16}H_{30}O_2$	16:1	butter, animal fats
Stearic	$C_{18}H_{36}O_2$	18:0	butter, animal fats
Oleic	$C_{18}H_{34}O_2$	18:1	olive, tall oil, peanut
Linoleic	$C_{18}H_{32}O_2$	18:2	safflower, sunflower
Linolenic	$C_{18}H_{30}O_2$	18:3	linseed

Separation of fats and oils from the original naturally occurring feedstock (animals and plants) is typically done by rendering, pressing or by using extracting solvent. Animal

fat can be obtained from carcasses by fat trimming and subsequent processing melting the fat and filtering the residual proteinaceous material and debris.

High oil content vegetable seeds can be processed with either mechanical pressing (yield 95-97 %) or solvent extraction (yield ≥99 %) for separation of oil. (Hasenhuettl 2016)

After achieving the desired pretreatment of feedstock (e.g bio-oil), it is ready for further processing. Even though bio-oils can be used directly for heat and electricity production, their utilization in transportation fuel and similar applications can require multiple process steps. The main reason is the high oxygen content of bio-oils, which has negative effect for the energy density, volatility, stability and other chemical properties of the bio-oil liquid. Examples of catalytic upgrading routes for bio-oil processing are demonstrated in Figure 2. (Serrano-Ruiz & Dumesic 2011)

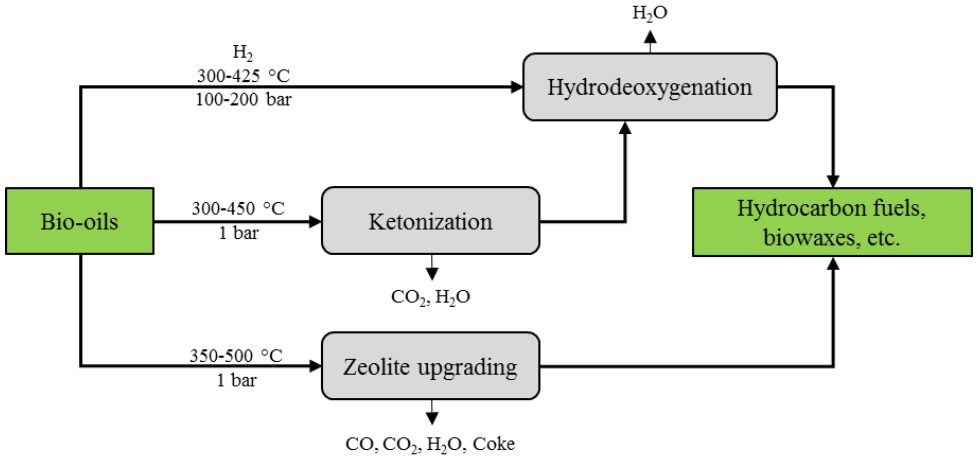

Figure 2 Examples of catalytic upgrading routes of biomass-derived oils into hydrocarbon fuels and other applications. (Serrano-Ruiz & Dumesic 2011, edited)

2.2 Main fatty acid reaction paths

Processing fatty acids into their corresponding hydrocarbons can be achieved by either decarboxylation, decarbonylation or hydrodeoxygenation. (Snåre et al. 2006) These catalyzed reaction experiments are typically investigated in semi-batch reactor or tubular fixed-bed reactors but they can also be performed in continuous mode reactors. Semi-batch studies are performed in stirred autoclave system. (Murzin & Simakova 2011)

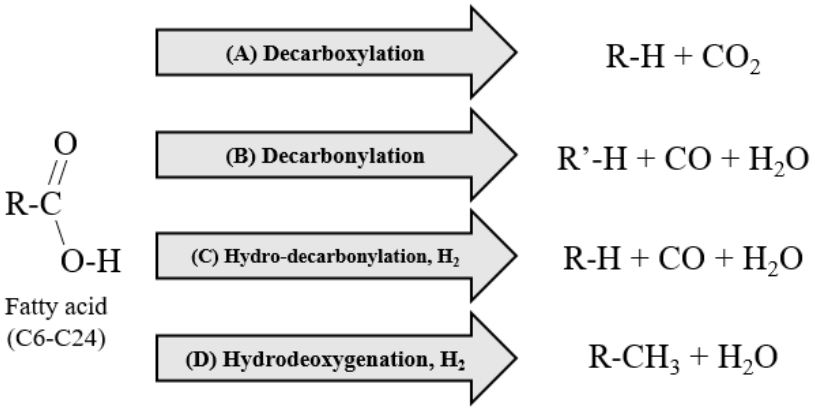

Figure 3 Different deoxygenation reaction paths of fatty acids to biodiesel: Decarboxylation (product with saturated alkyl group), decarbonylation, hydrogenation and hydrodeoxygenation. (Snåre 2006, edited)

2.2.1 Decarboxylation and decarbonylation

In fuel production, diesel-suitable n-Paraffins can be obtained from for example fatty acids through decarboxylation. Direct decarboxylation results in the elimination of carboxylic groups and formation of paraffin hydrocarbons and carbon dioxide. Alternatively, direct decarbonylation yields olefin hydrocarbon, carbon monoxide (CO) and water (H_2O). (Murzin & Simakova 2011)

According to Murzin and Simakova (2011), palladium and platinum based catalysts have been found to be effective in decarboxylation of fatty acids and their derivatives. Palladium catalyst on a carbon carrier is the most active and selective catalyst in the

case of stearic acid decarboxylation. Especially in deoxygenation, catalysts on a carbon carrier have the highest activity which is due to catalyst texture, porosity and specific surface. Other fundamental catalyst properties are its cost, durability and availability. (Wu et al. 2016)

2.2.2 Hydrogenation

When controlling the hydrogenation process it is important to select feasible raw materials and process conditions to achieve hydrogenated oils with specified properties. These conditions include e.g. temperature, hydrogen pressure and flow rate, residence time, and catalyst properties. Hydrogenation catalyst used in fats and oils industry is based mainly on nickel produced by BASF Catalysts or Johnson Matthey. Commonly used catalyst carrier is carbon and it's boundary layer type towards reaction components and inertness to side reactions of iso- and oligomerization mainly determine the effectiveness of the hydrogenation process (reaction rate, selectivity and formation of undesirable side products).

2.2.3 Deoxygenation

Laboratory scale deoxygenation, which includes decarboxylation and decarbonylation, has been studied in both semi-batch and continuous mode. Deoxygenation of fatty acids can be challenging due to low reaction rate and rapid catalyst deactivation. Additionally, operating with high melting point fatty acids C9:0 and over require proper heating for the complete reactor system (Bernas et al. 2010). In study by for example Snåre et al. (2006) this problem was managed with use of inert solvent. However, possible low solubility to solvents can also cause additional technical challenges.

3 KETONIZATION

In this chapter ketonization, its mechanisms and products further processing with hydrodeoxygenation is examined.

3.1 Ketonic decarboxylation

Ketones can be produced for example from fatty acids by ketonic decarboxylation in which two moles of carboxylic acid yields the so-called fatty ketone with water and carbon dioxide as side products. In addition to fatty acids, esters and specific aldehydes can be used as a feedstock. This process, being one of the oldest reactions known in organic chemistry, has been extensively studied through multiple different ketone syntheses. First major reported ketonization process was the production of acetone from calcium acetate as early as 1858. Nowadays ketones can be utilized in for example as solvents for example plastics or extraction and intermediate products in pesticide, herbicide and pharmaceutical production. General reaction for fatty acid ketonic decarboxylation is shown in Figure 3: (Renz 2005; Dooley 2004)

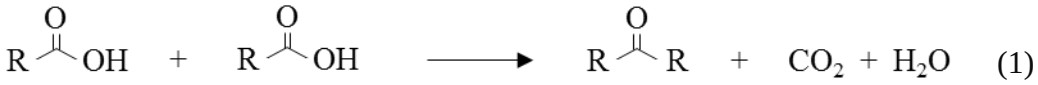

Figure 4 Chemical equation of ketonic decarboxylation (Renz 2005)

Based on the initial fatty acid composition in the feedstock, the formed ketones are either non-symmetric or symmetric. These reactions can be carried out in a continuous flow or batch type reactor. (Renz 2005)

3.2 Further processing with hydrodeoxygenation

Hydrodeoxygenation (HDO) is one of the most common methods to achieve oxygen removal from bio-oils. The process is carried out at high temperatures (< 300 °C), hydrogen pressures (100-200 bar) and typically either sulfide CoMo or NiMo catalyst is used. Sulfided catalyst is required in petrochemical industry to achieve simultaneous removal of sulfur and nitrogen. General hydrogenation reaction for ketones is shown in Figure 5. (Serrano-Ruiz & Dumesic 2011)

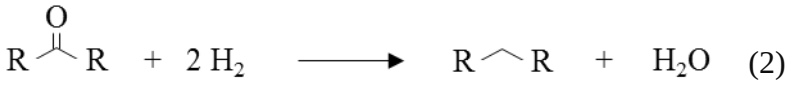

Figure 5 General reaction for hydrogenation of ketones.

After hydrogenation, ketones can serve as fuels or lubricant precursors (Oliver-Tomas et al. 2017)

3.3 Ketonization mechanisms

Despite of the extensive amount of research regarding ketonization, the ketonization mechanism is still in discussion. So-called radical mechanism, intermediate mechanism (β-keto acid) and concerted mechanism have been proposed. (Renz 2005) In the following chapters, the few of the most common mechanism theories are introduced.

3.3.1 Bulk and surface ketonization

It has been widely suggested that in the case of acetone formation from acetic acid, two different reaction routes exist: bulk and surface ketonization. Alkali earth oxides, such as MgO, CaO, BaO, SrO and CdO react strongly with acetic acid forming so-called

bulk carboxylate salts. (Pham et al. 2016;) These so-called bulk ketonization catalysts activate the decarboxylation by decomposition of the corresponding carboxylate salts. (Lu et al. 2017) The salt formation is possible due to basicity and the low lattice energy. The general reaction (at 150 °C) is shown below. (Lu et al. 2017; Pestman et al. 1997)

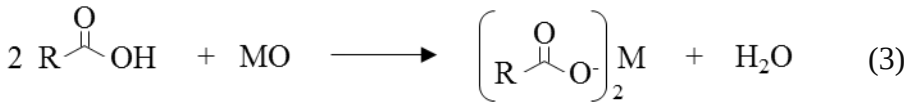

(3)

In higher temperatures (>150 °C), the decomposition reaction occurs either via

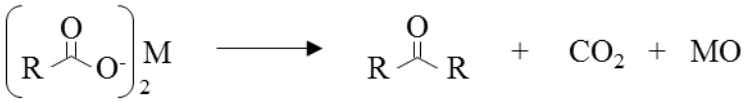

(4)

or via

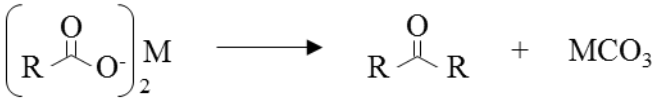

(5)

Comparably, with high lattice energy oxides the ketonization reaction takes place on the surface of the catalyst leaving the bulk structure of the catalyst unaltered. This type of catalysts include CeO_2, MnO_2, TiO_2, and ZrO2. The surface ketonization phenomenon is assumed to proceed via an intermediate which orientation is parallel to the surface, having chemical interactions with the catalyst via both the carboxyl group and the α-carbon of the alkyl group. The alkyl group of the intermediate can react with an adjacent carboxylate to yield the ketone. (Pestman et al. 1997) The intermediates formed in surface ketonization can include so-called β-ketoacids, ketene or anhydride. (Lu et al. 2017; Pestman et al. 1997)

3.3.2 Ketonization enabled by α-hydrogen

According to Pham et al. (2016), one of the main elements that appear in all surface ketonization related studies is the α-hydrogen, which has to exist in at least of the carboxylic acids involved in the reaction. The hydrogen is bonded to a carbon atom in the so-called α-position which is the first carbon atom attached to the functional group (carbonyl). The importance of α-hydrogen is based on its' relatively high acidity compared to other alkyl hydrogens. (Pham et al. 2016) Experimental carboxylic acid decarboxylation study by Pestman et al. (1997) with oxides of iron, titanium and vanadium confirmed that ketone production is related to the amount of α-hydrogen atoms in the acid.

Research conducted around the importance of α-hydrogen has enabled the development of several mechanism theories, for example intermediate mechanisms of ketene and β-ketoacid (Pham et al. 2016). These two mechanisms are presented in the following chapters.

3.3.3 Ketene-based mechanism

In this mechanism, acid forms a carboxylate intermediate on unsaturated metal site of the catalyst and subsequently, ketene intermediate is formed by dehydration reaction. The ketene ($R_2C=C=O$) couples with the alkyl group of the adsorbed carboxylate, forming the ketone. This mechanism is demonstrated with acetic acid in the Figure 6. (Faba et al. 2016; Pham et al. 2016)

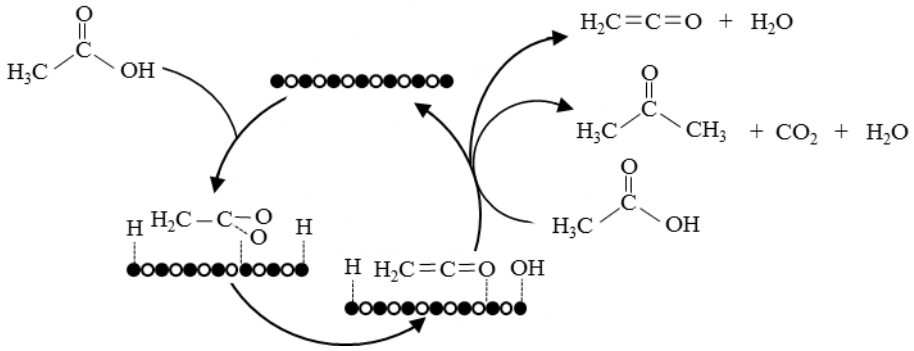

Figure 6 Mechanism scheme of acetic acid ketonization with ketene as intermediate. (Pham et al. 2013)

3.3.4 β-keto acid mechanism

Mechanism based on β-keto acid intermediate is considered as most valid in case of acetic acid ketonization. (Faba et al. 2016) This is due to the demonstrated important role of the intermediate in the reaction. The β-keto acid derives from coupling of enolate and carboxylate, in which enolate is a carboxylate with hydroxyl group bonded to carbon atom, which is connected to another carbon atom with a double bond. This mechanism is shown in Figure 7.

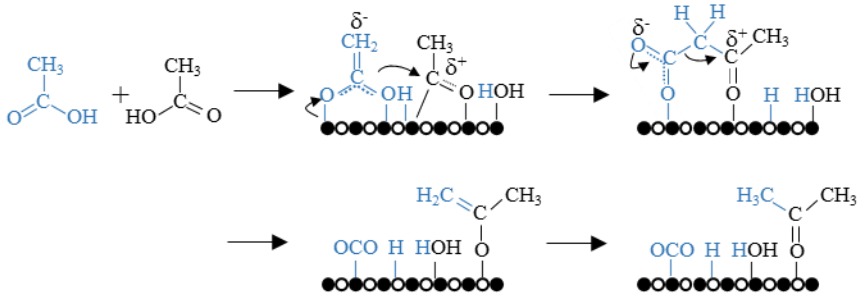

Figure 7 Decarboxylation reaction of acetic acid through mechanism based on β-keto acid as intermediate. (Pulido et al. 2013, edited)

5 MATERIALS AND METHODS

In this section, the used materials (feedstock, catalysts and gases) are discussed. Also, the reactor setup and run method is introduced in the later chapters.

5.1 Used materials

In this chapter, used feedstock, catalysts and gases are discussed.

5.1.1 Feeds

In the experimental study two different fatty acids were used for the main ketonization part: palmitic acid and oleic acid. This main feedstock is shown in Table I.

Table I Main feedstock and its properties

Name	Palmitic acid (PA, C16:0)	Oleic acid (OA, C18:1)
CAS no.	57-10-3	112-80-1
Manufacturer	Sigma-Aldrich	Sigma-Aldrich
Chemical formula	$C_{16}H_{32}O_2$	$C_{18}H_{34}O_2$
Purity	≥95 %	FCC
MW	256,42 g/mol	282,46 g/mol
Density 15 °C	873 kg/m3 (solid)	890 kg/m^3 (liquid)
Melting point	63,0 °C	13 – 14 °C
Boiling point	271,5 °C (100 mmHg)	194 – 195 °C (1,2 mmHg)

For the main ketonization tests 4 different samples were prepared from the two fatty acids above: 100% Palmitic acid, 90 % palmitic acid + 10 % oleic acid, 70 % palmitic acid + 30 % oleic acid, 50 % palmitic acid + 50 % oleic acid. The samples were prepared by weighing portions of the fatty acids to adjust the target distribution.

Additionally, two palmitic acid based esters were in use for individual ketonization tests: palmitic acid methyl ester (PAME) and palmitic acid ethyl ester (PAEE). Chemical properties of the feedstock is presented in Table II.

Table II Fatty acid esters for individual ketonization tests.

Name	Palmitic acid methyl ester (PAME)	Palmitic acid ethyl ester (PAEE)
CAS no.	112-39-0	628-97-7
Manufacturer	Sigma-Aldrich	Sigma-Aldrich
Chemical formula	$C_{17}H_{34}O_2$	$C_{18}H_{36}O_2$
Purity	≥97 %	≥95 %
MW	270,45 g/mol	284,48 g/mol
Density 15 °C	852 kg/m^3	857 kg/m^3
Melting point	35 °C	24 – 26 °C
Boiling point	185 °C (10 mmHg)	192 – 193 °C (10 mmHg)

5.1.2 HDO feedstock

As described in the previous chapter, main ketonization tests are carried out with four type of feeds: one pure palmitic acid and four different mixtures of palmitic acid and oleic acid. Additionally two special ethyl esters are tested for ketonization.

From the main ketonization tests, 4 ketonization products (introduced in chapter 5.1.1) are taken into further processing for hydrodeoxygenation (HDO) tests

5.1.3 Catalysts

Ketonization tests were performed with fresh titanium dioxide (TiO_2, anatase) as catalyst. The catalyst was grinded and sieved into specific sized powder to achieve ideal amount of contact of catalyst to the feed without needing to increase the catalyst to feed ratio in the limited reactor volume.

Before inserting the catalyst into the reactor in each experiment, the catalyst was dried in oven and afterwards in desiccator. Fresh dose of catalyst was used in all ketonization experiments to maintain as high as possible comparability between the tests since there is a risk of deactivation of catalyst. The appearance of the prepared TiO_2 catalyst can be observed in Figure 8.

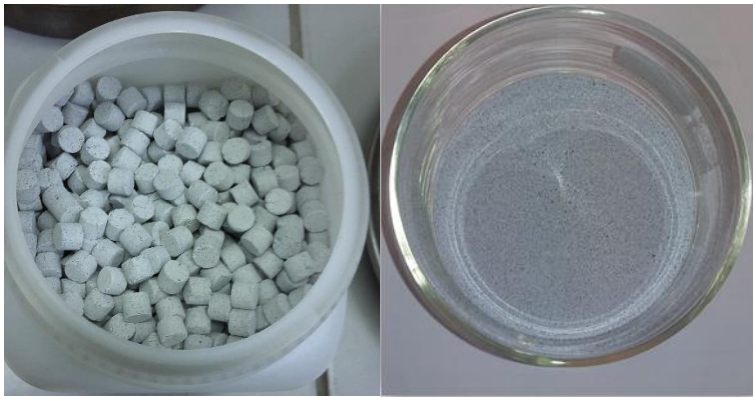

Figure 8 Fresh whole and grinded 0,15 – 0,30 mm TiO2 catalyst applied in ketonization.

The X-ray fluorescence analysis based composition of the catalyst is shown in the Table IV.

Table IV XRF composition of the TiO_2 ketonization catalyst

Aluminum, wt-%	0,08
Silica, wt-%	0,1
Phosphorus, wt-%	0,02
Sulfur, wt-%	0,2
Chloride, wt-%	<0,01
Potassium, wt-%	<0,01
Calsium, wt-%	0,01
Titanium, wt-%	56,52
Iron, wt-%	0,02

Additionally, catalyst pH, pore and crystal properties are shown in Table V.

Table V TiO_2 catalyst pH, pore and crystal properties.

pH	4
Crystallinity, %	94,1
Crystal size, Å	291
Pore diameter, Å	119,4422
Pore area, m^2/g	51,8
Pore volume, cm^3/g	0,155

In hydrodeoxygenation (HDO) part, conventional spent Nickel-Molybdene (NiMo) catalyst was applied for the experiments. For scheduling purposes, no fresh catalyst was used in HDO tests since the catalyst would have required pretreatment and main the goal of this part was just to achieve as complete as possible removal of oxygen from the ketones.

As for TiO_2 catalyst, also HDO catalyst was ground and sieved into specific size. Catalyst was also dried in 100 °C oven for 1 hour and kept in desiccator to decrease the effect of humidity on catalyst. The used catalyst is presented below in Figure 9.

Figure 9 Fresh (left) and spent NiMo-catalyst applied in the HDO experiments.

5.2 Experimental equipment and test procedures

The equipment used to carry out the semi-batch ketonization and hydrodeoxygenation tests was provided by 300 mL stirred reactor system from Parr Instrument Company. Heating, temperature, pressure, mixing speed and other process variables were managed with computer connected to Parr 4848B reactor controller. The main equipment consisted of 300 mL Hastelloy-made reactor, heater, stirrer motor and mixer, temperature and pressure sensors, safety rupture disk, heating cables and valves.

The reactor system was connected to three gas lines which were used in turns based on the type and phase of the experiment: the CO_2-bottle (30 kg, 50 bar) for ketonization, H_2 from gas manifold (200 bar) for HDO and He from gas manifold (200 bar) for pre-run leak testing. Both CO_2 and H_2 lines were connected into adjustable reduction valves and a gas measurement system to adjust the reactor pressure and gas flow rate. The pressure in the reactor was adjusted and held stable with pressure relief valve allowing the water, CO_2 and possible low boiling point side products to flow out towards cooled water trap container. From this container, gas was lead into Ritter drum-type gas volume meter and out of the fume hood by air exhaust.

All the pipelines in contact with either feedstock and product gas before the water trap had active heating to 150 °C with heating cables to minimize the risk of cold spots which may result in pipe clogging and a subsequent safety hazard due to the relatively high melting point of palmitic acid and ketone products. In case of uncontrollable pressure increase in the reactor, a 200 bar safety rupture disk was attached into the reactor holder. If needed, rupture disk would allow a safe pressure release enabling the reactor contents to flow into “dump” safety container through a heated pipeline.

The reactor controller was managed from the computer for temperature controlling, mixing speed and data logging. In case of major temperature rises or drops due to a process failure, high and low limit alerts were adjusted to allow operation in safe temperature zone and prevent solidification of the liquid in the reactor. The complete reactor system is presented as diagram in the Figure 10.

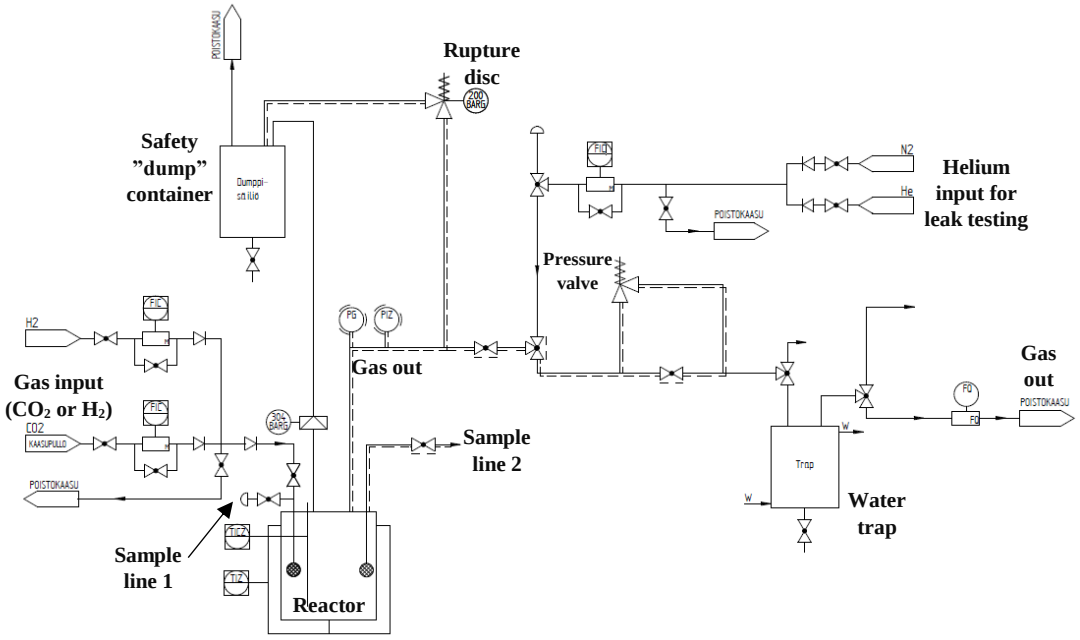

Figure 10 Simplified P&ID diagram of the Parr test equipment used in both ketonization and hydrodeoxygenation (HDO).

Main parts of the used Parr reactor system are shown in Figure 11.

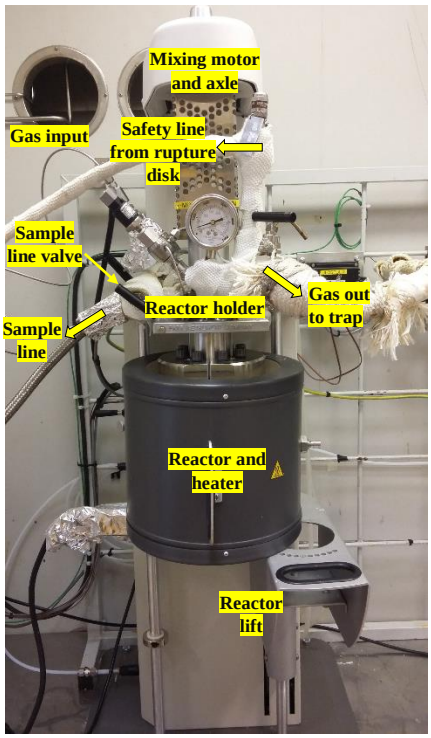

Figure 11 Parr reactor system used in this study.

As part of the pre-run preparations, reactor was held in 150 °C oven to maintain sufficient temperature on the reactor's inner surface when inserting the temperature sensitive feed with the catalyst. Additionally, a vortex breaker was placed into the reactor to achieve ideal mixing of the feed-catalyst mixture.

In the beginning of the experiments reactor was tightened with bolts and torque wrench into the so-called reactor clamps by simultaneously attaching it to the above reactor holder of the reactor system. The underside of the holder in contact with the interior of the reactor was equipped with 3 parts: a probe pocket for temperature sensor, a mixer axle with impeller and a 10 cm pipeline for the gas input and sampling. The end of the pipeline was also attached into a sintered filter to minimize the catalyst heading out of the reactor during sampling. In the following chapters, this pipeline is referred as "reactor line" for simplicity.

During the experiment's normal operation, needle valve (Valve A, Fig. 12) in contact with the pipeline connected to the reactor line were set so that the input gas flowed into the reactor line and out of the sintered filter inside reactor. After the filter, the gas bubbles flowed through the liquid and out of the reactor from output line hole in the upper part of the reactor.

The reactor's inner pressure, set at the beginning of the experiment, was utilized for sampling by using the reactor line in reverse direction compared to the normal operation. By closing the valve A, the pressure allowed the liquid to flow through the sinter filter and towards the valve B (Fig. 12) of the so-called sample line. By controlling this valve, a sample from the reactor could be obtained into a sample container at the end of the heated sample line. Due to the pipeline design, there was a risk of residual sample to be left into the sample line after obtaining a sample. This risk was managed by obtaining a "waste" sample from the sample line before the actual sample. During the sampling, the proper sample was discharged into a glass sample container held in an ice-filled decanter to handle the >300 °C liquid and prevent possible evaporation of low boiling point products. When sampling was finished, the sample line valve B was shut and the valve A opened to allow the gas flow into the reactor again while emptying the reactor line contents back into the reactor.

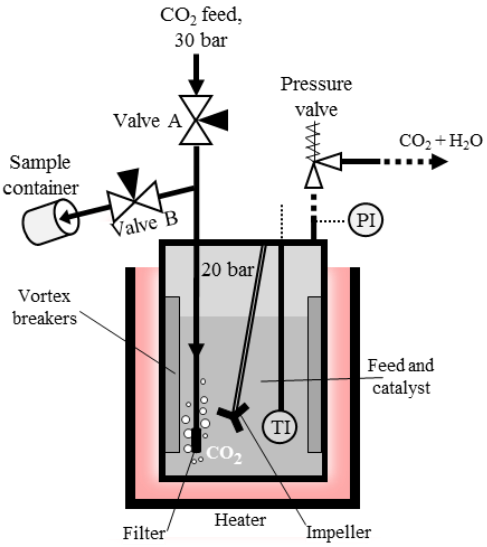

Figure 12 Simplified design of the reactor setup used in the ketonization experiments.

5.2.2 Herzog distillation

Distillation was performed with automated Herzog distillation unit for HDO experiment product samples. The goal of the distillation was to obtain comparable fraction of the long-chain paraffin containing samples from each experiment. Cut points for the distillation units were set based on external data received from simulated GC distillation. The distillation setup used in the experiments is shown in Figure 13.

Figure 13 Automatic distillation unit (Herzog) used in obtaining the final product samples.

5.2.3 Gas chromatography analysis

The liquid phase product samples were analyzed with an Agilent 7890A gas chromatograph (GC) with Agilent CP-Sil 5 CP column (10 m, 0,25 mm, 0,12 µm film). The device is presented in Figure 14.

Figure 14 Agilent 7890A with autosampler and heated agitator used in this study.

Samples (0,04 g) were prepared into Agilent 1,5 mL GC vials and dissolved into toluene which enabled injection of the samples. Samples were arranged into a heated agitator to maintain all the samples in liquid state. Helium was applied as carrier gas and samples were injected with automated sampler and 10 µL injector syringe in split mode with injection volume of 2 µL. Flame ionization detector (FID) with hydrogen and synthetic air was used as the detector for analytes in gas stream. Following oven temperature program was applied for all the samples (Table VI).

Table VII Agilent 7890A oven temperature ramps.

Rate, °C/min	**T, °C**	**Hold time, min**
-	60	2
8	310	0
5	340	30

Compound identification and graph integration was performed based on previous research studies' data with the same GC setup as well as external GC-MS identification data. An example of mixture of palmitic acid and oleic acid ketonization product chromatogram is shown in Figure 15.

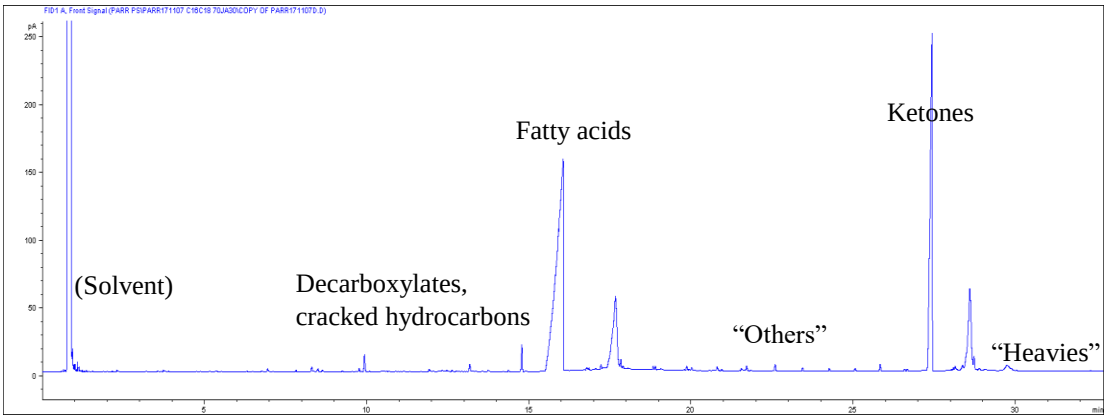

Figure 15 Example of GC chromatogram of a ketonization product sample.

For simplicity for the following sections, the so-called "heavies" zone is considered as "heavies fraction" which counts all the compounds above the known ketone range.

5.2.4 Additional analyses

The following additional analysis results were provided by Neste Oyj Analytical Laboratory: GPC, GC distillation, FIMS, IR and kinematic viscosity.

Gel permeation chromatography (GPC) analysis results provided by Neste Oyj Analytical Laboratory were used to provide additional information from the samples and support the information obtained from GC results. This technique, also known as size exclusion chromatography, separates the molecules based on their size (Agilent 2015). The results included the fractions of monomers, dimers, trimers.

Also, Gas Chromatography distillation (SimDist) was performed for the selected samples to obtain the boiling range distribution. Analysis provided the distribution for the boiling point area from 100 to 750 °C.

Field ionization mass spectrometry (FIMS) group analysis was used for characterization of different carbon number compounds from C13 to C66. Different fractions of organic compounds were calculated from the obtained GC spectrum.

Infrared spectroscopy (IR) analysis was performed with FTIR (Fourier-Transform Infrared Spectroscopy) instrument Thermo Nicolet iS10. The analysis is based on possibility to identify different absorb frequencies of chemical structures. IR analysis was applied after the HDO stage of the experiments to ensure that efficient oxygen removal has been achieved. The oxygen removal was studied by examining the IR spectrogram's section where carbonyl compounds are typically observed.

Kinematic viscosities at 80 °C and 100 °C were determined with glass capillary kinematic viscometer. Kinematic viscosity at 40 °C was determined by calculation based on the above-mentioned viscosity values due to the nature of the samples. Finally, viscosity index from the kinematic viscosities at 40 °C and 100 °C was determined.

6 RESULTS AND DISCUSSION

6.1 Gas chromatography results' background

Sampling was applied for studying the ketonic decarboxylation reaction (Chapter 3.1 of literature part). In the case of palmitic acid, two palmitic acid molecules formed a symmetrical C31 ketone (hentriacontanone). Additionally, simultaneous decarbonylation and decarboxylation occur as described in Figure 16. (Myllyoja 2017)

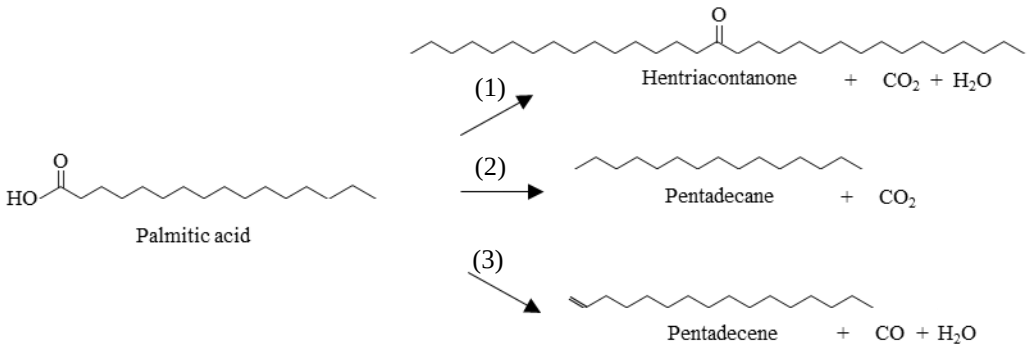

Figure 16 Examined reactions of palmitic acid: (1) ketonization, (2) decarboxylation and (3) decarbonylation (Myllyoja 2017)

In the case of mixed palmitic acid and oleic acid ketonization, additional symmetrical ketone was formed: pentatriacontanone (C35). Also formation of tritriacontanone (C33) through palmitic acid and oleic acid ketonization was observed. These main ketone products formed in the mixed feedstock experiments are shown in Figure 17.

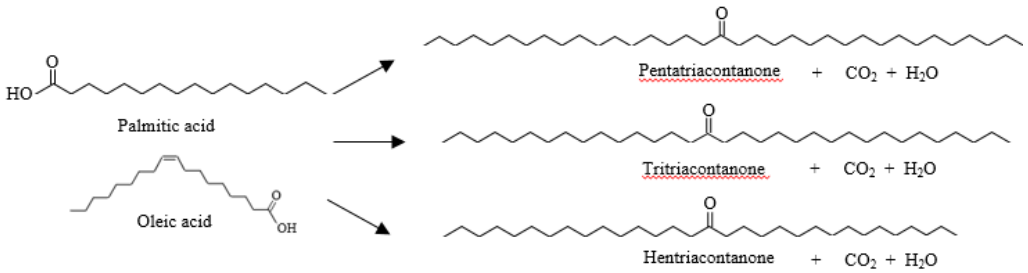

Figure 17 Main ketones formed from palmtic acid and oleic acid ketonization (Myllyoja 2017)

As seen in Fig. 16, each mole of ketone is assumed to form one mole of CO_2 and one mole of H_2O. The amount of water and carbon dioxide formed in the reaction was determined by calculation due to the challenges in collecting and measuring H_2O and measuring the formed CO2 from the gas stream. The calculation was performed based on the converted fatty acid amount.

6.2 Thermal stability test for C16:0

Thermal stability of palmitic acid (C16:0) was examined in the autoclave system to observe ketonization without catalyst. This experiment was carried out with 102,3 g of palmitic acid in 360 °C with 500 rpm mixing and 1,0 L/h continuous stream of CO_2. Reactor was heated to the target temperature (360 °C) and four samples were obtained from the reactor. The samples were analyzed with gas chromatography and the molar conversion was calculated based on the results (Table VII).

Table VIII Thermal stability test gas chromatography results for C16:0.

Sample	Reaction time, h from reaching 300 °C	C16:0, mol	C16:0 converted, mol	Conversion, %
Feed	-	0,387	-	0
1	1,067	0,373	0,014	0,4 %
2	2,117	0,351	0,036	6,4 %
3	6,217	0,287	0,100	11,8 %
4	7,100	0,232	0,155	27,1 %

Based on the results (Table VIII) thermal conversion of C16:0 is relatively low during first few hours of reaction time. With longer residence time (7,1 hours), 27 % conversion was achieved.

6.3 Ketonization run parameters' testing

Ketonization run parameters, such as catalyst size, mixing speed and feed-catalyst ratio were studied to optimize the process in terms of e.g. suitable reaction time. Additionally, basket-mode operation was tested to understand its' effect on ketonization and mass transfer.

Effect of catalyst size in palmitic acid ketonization was studied in the autoclave system in 350 °C and 20 bar with 500 rpm mixing and 1.0 L/h continuous stream of CO_2.

Palmitic acid vs. catalyst ratio was adjusted to 10,1. Following tests were performed (Table IX):

Table IX Effect of catalyst size in ketonization of palmitic acid: catalyst size in each experiment.

Experiment	Catalyst size
1	Full, 7 mm
2	Half, 3,5 mm
3	1-1.7 mm
4	0,15-0,35 mm

Three to four samples were obtained from each catalyst size experiment and the C16:0 converted amount was observed based on GC analysis. Results are shown in Appendix I and Figure 18 below.

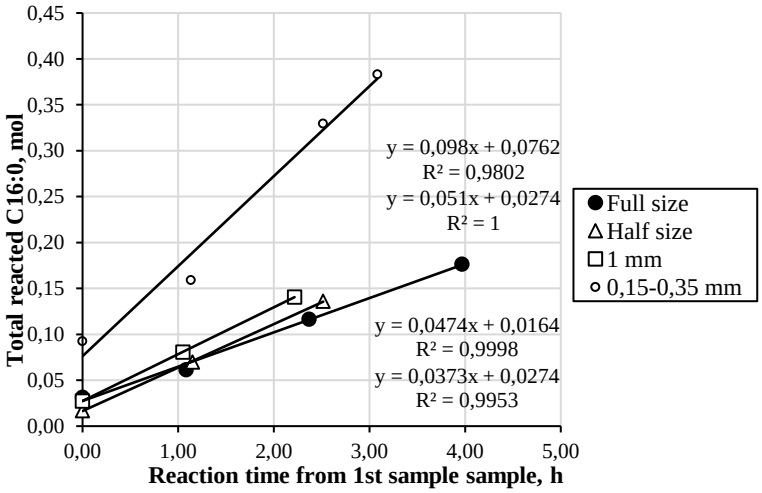

Figure 18 Total reacted C16:0 amount (mol) as function of reaction time from first sample in each catalyst size experiment (0,15-0,35; 1 mm-1,7 mm; half and full size).

Based on the Figure 18 linear plots C16:0 consumption doubles when catalyst size is decreased from 1-1,7 mm to 0,15-0,35 mm size. Results show that the C16:0 conversion builds as expected and is smaller with higher catalyst sizes. However, differences between other sizes (1-1,7 mm, half and full size) is relatively small. The clear difference between 1-1,7 mm and 0,15-0,35 mm can occur due to significant increase of catalyst surface area when powder-like catalyst is used.

Different mixing speeds were also tested to study its' effect on reaction. Mixing speeds tested were 100 rpm, 270 rpm and 540 rpm. Results of these experiments are shown in Figure 19.

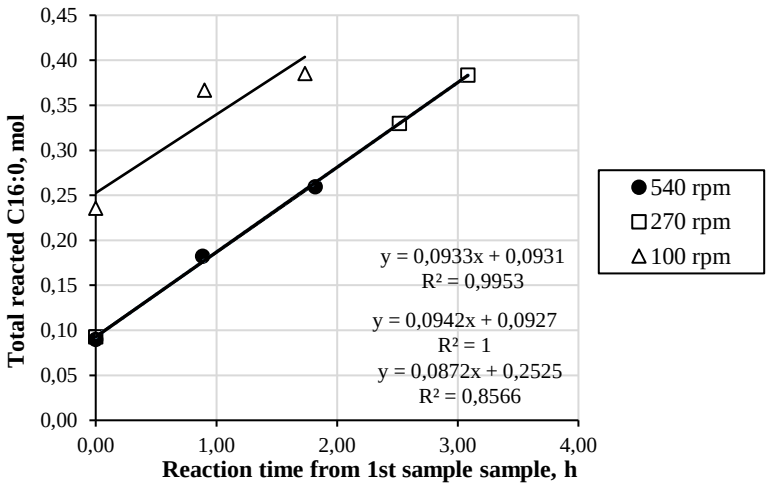

Figure 19 Total reacted C16:0 in mol units as function of reaction time from 1st sample in experiments with different mixing speeds.

As seen in Figure 19, mixing speed of 100 rpm shows more irregular development in total reacted C16:0 than the other experiments. This might be due to too low mixing speed and therefore reactor contents were not ideally mixed especially during sampling. With mixing speeds of 270 and 540 rpm highly similar results were obtained in terms of development of reacted C16:0 amount. This indicates that mixing speeds in this range may not have a clear effect on the conversion of the feedstock. However, the

higher mixing speed was chosen for further experiments to ensure reactor mixing is as ideal as possible in all experiments.

Finally, different feed to catalyst -ratios (F/C) were tested with one of the test performed in catalyst basket instead of slurry. Experiment with 540 rpm mixing speed and F/C ratio of 10 from previous section was compared to slurry experiment with F/C ratio of 15 and catalyst basket experiment of F/C = 31. All the experiments were performed in 350 °C and 20 bar. Results from this test series is shown in Figure 20.

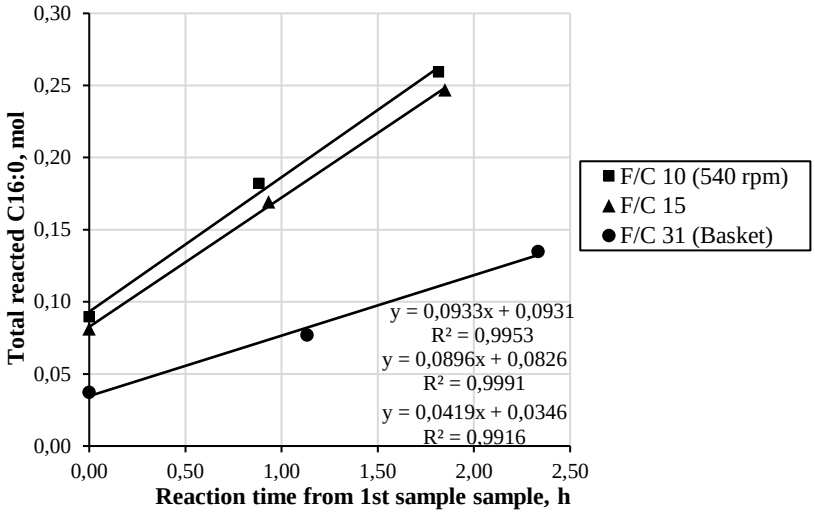

Figure 20 Total reacted C16:0 amount (mol) as function of reaction time from 1st sample in experiments with variable feed-catalyst ratio. Experiment with highest F/C ratio (31) was performed with catalyst basket (1-1,7 mm catalyst size) and lower F/C ratio samples with 0,15-0,35 mm size catalyst.

According to the data, results seem reasonable in terms of conversion development when feed-catalyst ratio is decreased. The results were used as a basis for further evaluation of process parameters for C16:0 and C18:1 mix tests for example in optimizing the reaction time and sample amount. Experiments are not throughout comparable since basket-mode experiment had to be performed with higher amount of feed to obtain sufficient height for the liquid phase to submerge the basket completely.

6.4 Effects of temperature and pressure

The effect of temperature and pressure for the conversion and ketonization of palmitic acid (C16:0) was studied with 3 different temperatures and pressures. TiO_2 (size 0,15-0,35 mm) was weighed 7 g as catalyst for the reaction and CO_2-feed of 1.0 L/h was used. The following experiments were performed (Table X):

Table X Experiments performed for the study of reaction conditions for palmitic acid ketonization.

Experiment	T, °C	p, bar
1	335	10
2	335	20
3	345	15
4	345	17
5	355	10
6	355	20

During each selected reaction conditions 4 samples were obtained from the reactor. Sampling interval was chosen so that all the tests would focus in the early conversion of the palmitic acid to maintain ideal comparability. All the samples were ran through GC analysis to study the difference of C16:0 conversion and ketone (C30 ketone) formation in different reaction conditions. The analysis results for different temperature (335 °C 20 bar, 345 °C 17 bar, 355 °C 20 bar) tests are shown in Table XI and Figure 21. High selectivity is observed from the results as major part of the reacted palmitic acid converts into the main ketone product (hentriacontanone). During the examined reaction time possible cracking, residual ketonization intermediates, and formation of heavy long-chain products are relatively stable. However, this result can occur due to the high catalyst initial activity and low total C16:0 conversion during the examined, relatively short reaction time.

Table XI Gas chromatography results for experiments (335 °C 20 bar, 345 °C 17 bar and 355 °C 20 bar)

335 °C 20 bar				
T	1	2	3	4
Time, h from sample 1	0	0,63	1,35	1,84
C16:0, A-%	87,5	83,3	78,6	74,8
C15-C15ketone, A-%	8,9	13,1	17,5	21,2
Others, A-%	3,6	3,6	3,9	4,0
345 ° 17 bar				
Sample	1	2	3	4
Time, h from sample 1	0	0,46	0,94	1,38
C16:0, A-%	87,7	83,1	77,5	73,7
C15-C15ketone, A-%	8,5	13,5	18,7	22,3
Others, A-%	3,8	3,4	3,8	4,0
355 °C 20 bar				
Sample	1	2	3	4
Time, h from sample 1	0	0,31	0,63	0,99
C16:0, A-%	71,6	64,8	58,9	51,1
C15-C15ketone, A-%	23,8	30,0	34,9	42,4
Others, A-%	4,6	5,2	6,2	6,5

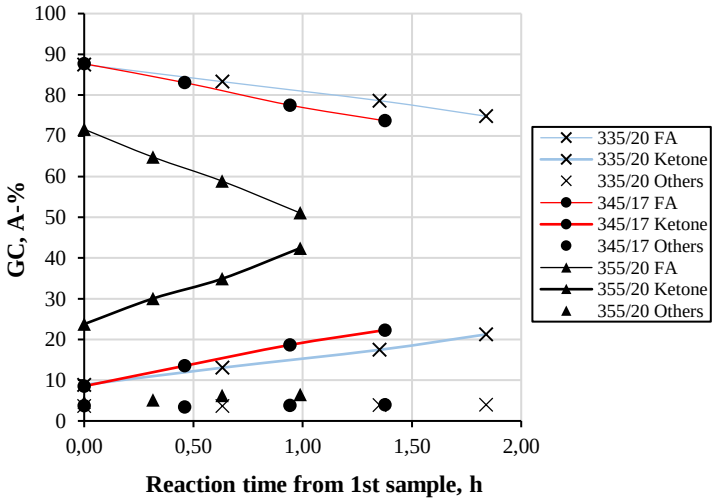

Figure 21 Selected gas chromatography results (Area-%) for the palmitic acid ketonization experiments 335 °C 20 bar, 345 °C 17 bar, 355 °C 20 bar. Abbreviations: FA = Palmitic acid, Ketone = Hentriacontanone, Others = all other identified compounds.

Based on the results the fatty acid conversion develops expectedly when rising the reaction temperature from 335 °C to 345 ° and 355 °C. The effect of temperature on the conversion of C16:0 can be observed in the Figure 22. The x-axis was selected to enable straightforward comparison between the experiments which all had variations in for example reactor heating velocity. As seen from the figure, palmitic acid conversion development almost doubles when temperature is increased from 335 °C to 345 °C and to 355 °C.

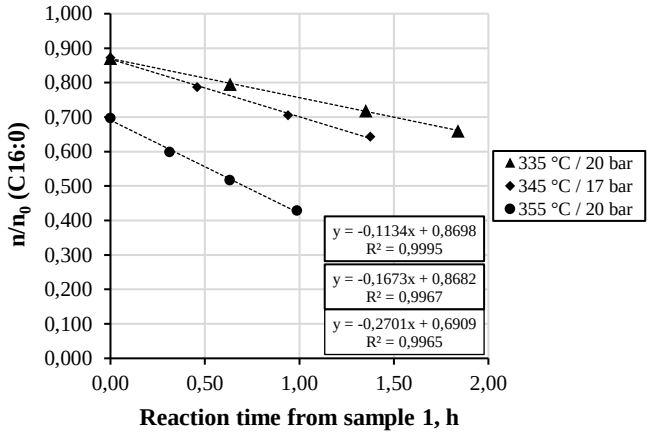

Figure 22 Effect of temperature (335, 345, 355 °C) for palmitic acid (C16:0) conversion as a function of reaction time calculated from the 1st sample.

Effect of pressure was studied with two pressure values: 10 and 20 bar for the temperatures 335 °C and 355 °C. Based on the results no significant effect was observed in the palmitic acid conversion or the main ketone product (Hentriacontanone) formation. The results for the both C16:0 conversion and C15-C15 -ketone formation can be seen from the Figures 23 and 24. Linear fit for the both compounds data set was added to observe the differences between the two pressure experiments.

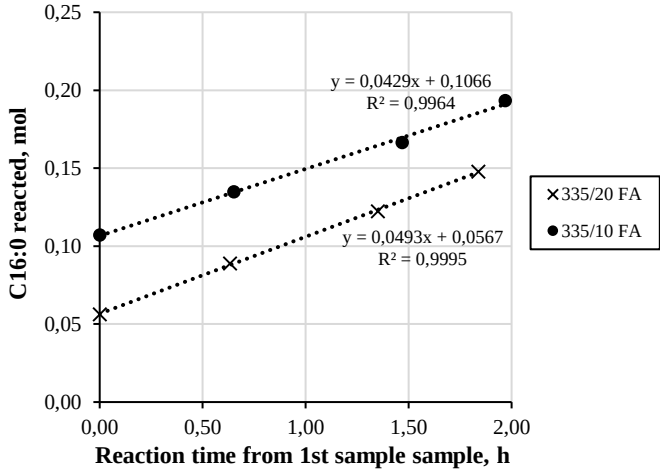

Figure 23 Effect of pressure on palmitic acid ketonization: C16:0 conversion development in 335 °C.

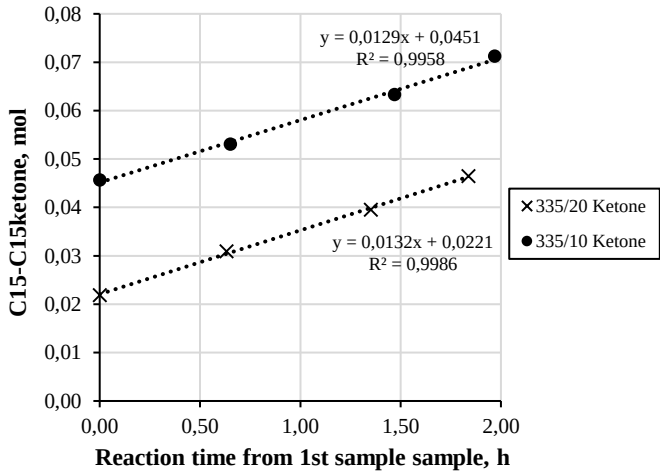

Figure 24 Effect of pressure (10 vs. 20 bar) for palmitic acid (C16:0) ketonization to hentriacontanone (C15-C15ketone) in 335 °C.

As seen in Fig 23 and 24, results of experiments in the pressures 10 and 20 bar do not indicate clear difference in the development of the ketonization reaction in 335 °C. The development of C16:0 conversion and C15-C15 -ketone formation is slightly increased in 20 bar pressure. However, the small variations heating stability and possible errors originating from the gas chromatography analysis can influence the results.

The development of C16:0 conversion and C15-C15 -ketone formation in 355 °C (pressures 10 and 20 bar) can be seen in Figures 25 and 26.

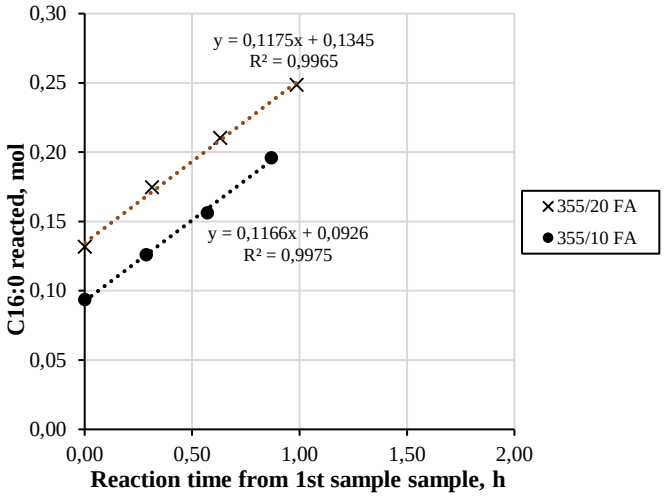

Figure 25 Palmitic acid conversion in 355 °C in pressures 10 and 20 bar.

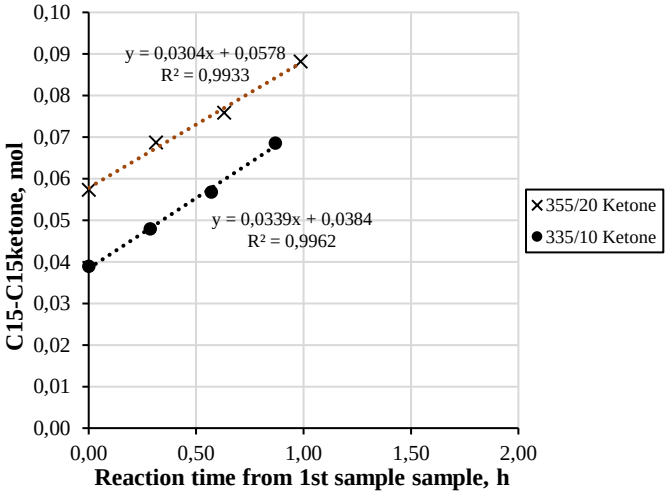

Figure 26 Effect of pressure (10 vs. 20 bar) for palmitic acid ketonization to hentriacontanone in 355 °C.

As the previous results, also the experiments in 355 °C indicate that pressure does not have a visible effect in the development of fatty acid conversion or ketone formation.

Based on these observations, pressure in the selected range in the chosen conditions can be considered as insignificant factor in ketonization of palmitic acid.

6.5 C16:0 and C18:1 ketonization tests

Palmitic acid ketonization was also studied in presence of double bonds, precisely oleic acid (C18:1). The following experiments were carried out (Table XII).

Table XII Experiments carried out with either pure palmitic acid or mixture of palmitic acid and oleic acid.

Run	C16:0, w-%	C18:1, w-%
1	99,7	0
2	90,4	8,4
3	71,4	25,5
4	53,0	42,2

Each mixture experiment was performed twice to obtain sufficient amount of product for further processing in hydrodeoxygenation (HDO) experiments. The pure 100 % C16:0 ketonization product was combined from multiple experiments and therefore its' results are not presented in this chapter. All experiments were carried out in 360 °C, 20 bar and with F/C ratio of 16,5. The gas chromatography results for each of the mixtures first ketonization experiment are shown in Table XIII.

Table XIII Gas chromatography results for each sample from different C16:0 + C18:1 mixture ketonization experiments.

90 % C16:0, 10 % C18:1				
Sample	1	2	3	4
Time from sample 1, h	0	1,3	3,4	4,0
C16:0, A-%	63,2	37,8	7,0	0,9
C18:1, A-%	4,1	2,0	0,3	0,1
C15-C15ketone, A-%	20,3	41,0	64,4	68,6
C15-C17ketone, A%	2,4	4,4	5,4	5,4
C17-C17ketone, A-%	0,1	0,0	0,4	0,4
FA-area and smaller, A-%	7,2	9,7	11,6	12,1
Others, ketone zone, A-%	2,0	3,8	7,4	8,0
Heavy fraction, A-%	0,6	1,3	3,6	4,6
70 % C16:0, 30 % C18:1				
Sample	1	2	3	4
Time from sample 1, h	0	1,1	2,8	4,7
C16:0, A-%	56,4	37,5	18,0	1,3
C18:1, A-%	18,1	10,1	4,1	0,3
C15-C15ketone, A-%	9,7	23,9	38,0	48,2
C15-C17ketone, A%	4,0	8,9	12,5	13,5
C17-C17ketone, A-%	0,6	1,2	1,6	1,8
FA-area and smaller, A-%	8,0	11,9	14,3	14,7
Others, ketone zone, A-%	2,3	5,3	9,0	14,0
Heavy fraction, A-%	0,9	1,4	2,4	6,1
50 % C16:0, 50 % C18:1				
Sample	1	2	3	4
Time from sample 1, h	0	1,2	2,5	3,9
C16:0, A-%	40,6	27,8	12,5	2,1
C18:1, A-%	25,8	15,8	5,8	0,2
C15-C15ketone, A-%	7,3	15,6	25,1	31,5
C15-C17ketone, A%	6,6	12,3	17,2	18,3
C17-C17ketone, A-%	1,8	3,1	4,1	4,4
FA-area and smaller, A-%	12,3	15,5	18,8	18,7
Others, ketone zone, A-%	3,9	7,5	12,5	17,3
Heavy fraction, A-%	1,7	2,5	4,0	7,0

According to the obtained data higher C18:1 fraction in the initial feedstock results in slightly higher cracking and formation of compounds heavier than the identified ketones. This phenomenon can be seen throughout the reaction in each sample and it supports the theory that the differences in the experiments are truly originating from the fatty acid composition in the feedstock. As expected, higher C18:1 fraction also produces wider distribution of products identified in the ketone area, simultaneously reducing the total amount of main ketones (C15-C15, C15-C17 and C17-C17) compared to the ketonized feedstock containing less than 10 % C18:1.

6.6 Other feedstock ketonization (FAME and FAEE)

In addition to C16:0 and C18:1, ketonization with TiO_2 as catalyst was studied with other fatty acid esters: palmitic acid methyl ester (methyl palmitate) and palmitic acid ethyl ester (ethyl palmitate). Reaction conditions were selected based on the previous experiments with palmitic acid ketonization and four samples were obtained from the reactor during the experiment. Each sample was analyzed with gas chromatography and these results are shown in Table XIV for methyl palmitate ketonization and Table XV for ethyl palmitate ketonization.

Table XIV Methyl palmitate ketonization results from gas chromatography analysis.

Sample	1	2	3	4
Time from sample 1, h	0	1,4	2,2	3,5
Methyl palmitate and C16:0, A-%	38,4	12,2	3,4	1,3
C15-C15ketone, A-%	40,4	56,7	57,3	45,4
FA-area and smaller, A-%	12,7	13,9	15,7	18,8
Others, ketone zone, A-%	6,1	10,5	14,2	21,7
Heavy fraction, A-%	2,5	6,7	9,5	12,8

Table XV Ethyl palmitate ketonization results from gas chromatography analysis. Last sample was obtained after reactor cooling phase (*).

Sample	1	2	3	4
Time from sample 1, h	0	2,0	2,9	*
Ethyl palmitate and C16:0, A-%	64,0	21,3	9,8	4,1
C15-C15ketone, A-%	20,4	48,2	58,3	59,5
FA-area and smaller, A-%	10,7	17,7	16,3	19,3
Others, ketone zone, A-%	4,1	10,3	12,8	13,2
Heavy fraction, A-%	0,8	2,4	2,9	3,9

The end products obtained after cooling of the reactor were also analyzed with GPC. Results can be seen in Table XVI.

Table XVI Methyl palmitate and ethyl palmitate ketonization end products' GPC results.

Fraction	Methyl palmitate	Ethyl palmitate
Parafins	12,2	17,5
Dimers	65,2	76,4
Trimers	15,6	5,3
Tetramers	7,0	0,9

Based on the above results, main product for both methyl palmitate and ethyl palmitate is C15-C15 -ketone. This result confirms that ketonization of C16 based fatty acid esters is possible and produces similar main compound as the palmitic acid. However, relatively high heavy product formation especially in the case of methyl palmitate can be detected. Methyl palmitate ketonization and its further reactions also produce other so far unidentified products in the ketone zone, almost half of the amount of main ketone.

6.7 Hydrodeoxygenation tests

Selected ketonization products were mixed to obtain enough sample for further hydrogenation (HDO) tests. The following 4 ketonization product samples were prepared: 100% C16:0, 90 % C16:0 + 10 % C18:1, 70 % C16:0 + 30 % C18:1 and 50 % C16:0 + 50 % C18:1. Each sample were combined from two different ketonization runs. HDO experiments were performed in 310 °C, 90 bar and with 20 L/h H_2.

The combined samples for HDO were analyzed with GC and these results are shown in Table XVII.

Table XVII Combined ketonization product batches for hydrodeoxygenation: 1) Pure C16:0 2) 90 % C16:0 + 10 % C18:1, 3) 70 % C16:0 + 30 % C18:1 and 4) 50 % C16:0 + 50 % C18:1 based ketonization product.

Batch	1	2	3	4
Below Fatty acids, A-%	4,9	10,2	9,7	10,8
Fatty acids, A-%	0,3	0,1	1,8	4,8
Ketone zone, A-%	88,9	82,4	80,7	71,9
Heavy fraction, A-%	5,9	6,3	6,1	9,7

After each hydrodeoxygenation experiment, catalyst and liquid were separated first by decantation and finished with hot filtration through membrane filter. The appearance of the filtered products can be observed in the Figure 27.

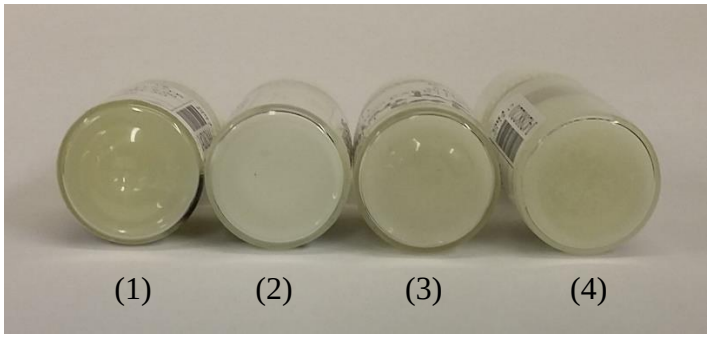

Figure 27 Color comparison of HDO products from C16:0 and C16:0+C18:1 (90/10, 70/30, 50/50) ketonisation experiments.

The hydrogenated samples were analyzed with simulated gas chromatography distillation (Simdist) to obtain the boiling point range distribution to allow the estimation of the cut point for Herzog distillation. The Simdist results are shown below in Table XVIII.

Table XVIII Simdist results for each sample.

Batch	1	2	3	4
Fraction, bp <381 °C	6,1	12,1	14,6	19,7
Fraction, bp 381-547,57 °C	85,4	80,1	77,6	68,5
Fraction, bp >547,57 °C	8,5	7,8	7,8	11,8

The target of the cut point was to separate the so-called light fraction from the biowax product and to minimize their effect for the viscosity results.

After the distillation, further analyses were performed. The analysis results (Simulated GC distillation, GC and GPC) are presented in the Table XIX

Table XIX GC, GPC and Simulated GC distillation results for each distilled HDO product.

Batch	1	2	3	4
<C23	1,6	2,9	3,8	4,6
C23-C45 fraction	96,6	93,9	91,1	88,0
>C45	1,8	3,2	5,1	7,4
Monomers, A-%	1	2,1	2,6	3,9
Dimers, A-%	91,6	87,1	82,4	75,0
Trimers, A-%	5,8	7,8	10,1	13,6
Tetramers, A-%	1,6	3	4,9	7,5
Simdist,, <C23	<1	2,11	2,65	3,18
Simdist, C23-C45	92,6	92,6	88,1	82,2
Simdist, >C45	7,4	5,3	9,3	14,7

As seen from the results, the trimer and tetramer fraction increases as the amount of larger compounds increases due to the oleic acid ketonization and hydrodeoxygenation derivatives.

Additionally, samples were also analyzed with field ionization mass spectrometry (FIMS). Results are shown in Table XX.

Table XX FIMS results for each final biowax product batch.

Batch	1	2	3	4
Paraffins, %	99.5	97.3	94.7	86.9
Mononaphtenes, %	0.5	2.7	5.3	13.0
C29, %	0.4	0.5	0.1	0.3
C31, %	98.4	91.8	77.3	58.0
C33, %	0.3	4.6	17.1	26.7
C35, %	0	0	0	1.7

Finally, kinematic viscosity of the samples was determined in 3 temperatures: theoretically in 40 °C and experimentally in 80 °C and 100 °C. Based on these values, viscosity index (VI) was determined. The results can be seen in Table XXI.

Table XXI Viscosity results for each final product batch.

Batch	1	2	3	4
Viscosity 40 °C (calc), mm^2/s	24,04	25,68	28,82	33,86
Viscosity, 80 °C, mm^2/s	6,779	7,086	7,637	8,503
Viscocity 100 °C, mm^2/s	4,728	4,915	5,258	5,774
Viscosity index	116,3	116,0	114,8	111,8

Based on the results, C33 paraffin and higher compound composition has a notable effect on the viscosity values. Viscosity index decreases by 4 units when (mainly) C31 paraffin product (batch 1) is compared to the batch 4 with C33 paraffins and higher compounds.

8 CONCLUSIONS

In the experimental part, semi-batch catalytic test runs were carried out with fatty acids C16:0 and C18:1 as well as fatty ester acids. Different factors affecting the batch experiment were studied. Finally, chosen batches of mixed fatty acid ketonization tests (Feedstock C16:0/C18:1 ratios 100/0, 90/10, 70/30 and 50/50) were ran through hydrodeoxygenation to obtain biowax product and study its' properties.

Mixed fatty acid ketonization tests from higher feedstock C16:0 percentage to lower yielded 89; 82; 81 and 72 % ketone zone products based on GC analysis. Respectively, these tests heavy fraction products with percentages 5,9; 6,3; 6,1 and 9,7 %. These batches were processed further with hydrodeoxygenation and distillation to paraffinic hydrocarbon biowax product. Based on FIMS analysis, the final product batches consisted of 98; 92; 77 and 58 % of C31 paraffin which was the direct hydrodeoxygenated product from palmitic acid ketonization to C15-C15 -ketone. Comparably, C33 paraffin fraction, yielding from palmitic acid and oleic acid ketonization product C15-C17 -ketone, in these experiments was 0, 5, 17 and 27 %. Notable in the paraffin analysis in these experiments was that according to FIMS, only 0 to 2 % of C35 paraffin (HDO product of C17-C17 ketone from ketonization of two oleic acid molecules) was identified after HDO. However, this type of result may occur due to the possible unstable nature ketones formed from unsaturated fatty acids, in this case oleic acid. Respectively, the GC-based heavy fraction (products >C45 paraffin) was 2; 3; 5 and 7 % for each batch of distilled biowax product. The wider ketone product composition and the higher heavy fraction had an expected effect on the viscosities of the products, increasing the viscosity at 100 °C from 4,7 to 5,8 mm^2/s when compared from pure C16:0 based product to the 50/50 C16:0 and C18:1 mix based product.

Fatty acid ester ketonization tests indicated that especially fatty acid ethyl ester (palmitic acid ethyl ester) has potential for feedstock for palmitic acid type

ketonization. Based on GC analysis fatty acid esters go through similar pathway as fatty acids to form C15-C15 -ketone with relatively high selectivity.

Based on the experiments and their analysis results, logical and wide scale of data could be obtained with laboratory scale semi-batch ketonization and further HDO experiments. Results indicate that this method can work as important base for example kinetic studies and pre-testing for different feedstocks to provide data possibly needed for higher-scale tests or continuous-mode operation. However, further optimization is needed to manage the challenges with temperature stabilization with the reactor heater.

REFERENCES

Agilent, 2015, An Introduction to Gel Permeation Chromatography and Size Exclusion Chromatography, [online], Available at: https://www.agilent.com/cs/library/primers/Public/5990-6969EN%20GPC%20SEC%20Chrom%20Guide.pdf [accessed January 20th, 2018]

Bernas, H., Eränen, K., Leino, A-R., Kordás, K., Myllyoja, J., Mäki-Arvela, P., Salmi, T., Murzin, D., 2010, Deoxygenation of dodecanoic acid under inert atmosphere, Fuel: The Science and Technology of fuel and energy, Vol. 89, pp 2033-2039

Climent, M., Corma, A., Iborra, S., 2014, Conversion of biomass platform molecules into fueld additives and liquid hydrocarbon fuels, Green Chem., Vol. 16, pp. 516-547

Dooley, K., 2004, Catalysis of Acid/Aldehyde/Alcohol Condensations to Ketones, In: Spivey, J., Roberts, G. (Editors), Catalysis, Vol. 11, pp 293-319

Faba, L., Díaz, E., Ordóñez, S., 2016, Base-Catalyzed Reactions in Biomass Conversion: Reaction Mechanisms and Catalyst Deactivation, In: Schlaf, M., Zhang, Z., (Editors), Reaction Pathways and Mechanisms in Thermocatalytic Biomass Conversion I, pp. 87-122

Hasenhuettl, G., 2016, Fats and Fatty Oils, In: Seidel, A. (Editor), Kirk-Othmer Encyclopedia of Chemical Technology, John Wiley & Sons, pp. 1-37

Lu, F., Jiang, B., Wang, J., Huang, Z., Liao, Z., Yang, Y., Zheng, J., Promotional effect of Ti doping on the ketonization of acetic acid over a CeO_2 catalyst, 2017, RSC Adv., Vol. 7, pp. 22017-22026

Miao, C., Marin-Flores, O., Davidson, S., Li, T., Dong, T., Gao, D., Wang, Y., Garcia-Pérez, M., Chen, S., Hydrothermal catalytic deoxygenation of palmitic acid over nickel catalyst, Fuel: The Science and Technology of fuel and energy, Vol. 166, pp 302-308

Mittelbach, M., 2015, Fuels from oils and fats: Recent developments and perspectives, Eur. J. Lipid Sci. Technol., Vol. 117, pp. 1832-1846

Murzin, D., Simakova, I., 2011, Catalysis in biomass Processing, Catalysis in Industry, Vol. 3, pp. 218-249

Oliver-Tomas, B., Renz, M., Corma, A., 2017, High Quality Biowaxes from Fatty Acids and Fatty esters: Catalyst and Reaction Mechanism for Accompanying Reactions, Ind. Eng., Chem. Res., xxx

Myllyoja, J., 2017, personal discussion

Pestman, R., Koster, R., van Duijne, J., Pieterse, J., Ponec, V., 1997, Reactions of Carboxylic Acids on Oxides: 2. Bimolecular Reaction of Aliphatic Acids to Ketones, Journal of Catalysis, Vol. 168, pp. 265-272

Pham., T., Sooknoi, T., Crossley, S., Resasco, D., 2013, Ketonization of Carboxylic Acids: Mechanisms, Catalysts, and Implications for Biomass Conversion, ACS Catal., Vol. 3, pp. 2456-2473

Pulido, A., Oliver-Tomas, B., Renz, M., Boronat, M., Corma, A., 2013, Ketonic Decarboxylation Reaction Mechanism: A Combined Experimental and DFT Study, ChemSusChem, Vol. 6, pp. 141-151

Renz, M., 2005, Ketonization of Carboxylic Acids by Decarboxylation: Mechanism and Scope, Eur. J. Org. Chem., pp. 979-988

Serrano-Ruiz, J, Dumesic, J., 2011, Catalytic routes for the conversion of biomass into liquid hydrocarbon transportation fuels, Energy Environ. Sci., Vol. 4, pp. 83-99

Snåre, M., Kubičková, I., Mäki-Arvela, P., Eränen, K., Murzin, D., 2006, Continuous Deoxygenation of Ethyl Stearate: A Model Reaction for Production of Diesel Fuel Hydrocarbons, In: Schmidt, S. (Editor), Catalysis of Organic Reactions, 2007, Taylor & Francis Group, LLC, pp 415-425

Snåre, M., 2006, Licentiate thesis: Catalytic deoxygenation of renewable sorurces – A novel method for production of biodiesel, Laboratory of Industrial Chemistry, Åbo Akademi University

Sigma Aldrich, 2018, Ethyl palmitate safety data sheet, [online], Available at: https://www.sigmaaldrich.com/MSDS/MSDS/DisplayMSDSPage.do?country=FI&language=EN-generic&productNumber=W245100&brand=ALDRICH&PageToGoToURL=%2Fsafety-center.html [accessed January 20th, 2018]

Sigma Aldrich, 2018, Methyl palmitate safety data sheet, [online], Available at: https://www.sigmaaldrich.com/MSDS/MSDS/DisplayMSDSPage.do?country=FI&language=EN-generic&productNumber=W509531&brand=ALDRICH&PageToGoToURL=%2Fsafety-center.html [accessed January 20th, 2018]

Sigma Aldrich, 2018, Oleic acid safety data sheet, [online], Available at: https://www.sigmaaldrich.com/MSDS/MSDS/DisplayMSDSPage.do?country=FI&language=EN-generic&productNumber=W281506&brand=ALDRICH&PageToGoToURL=%2Fsafety-center.html [accessed January 20th, 2018]

Sigma Aldrich, 2018, Palmitic acid safety data sheet, [online], Available at:

https://www.sigmaaldrich.com/MSDS/MSDS/DisplayMSDSPage.do?country=FI&language=EN-generic&productNumber=W283207&brand=ALDRICH&PageToGoToURL=%2Fsafety-center.html [accessed January 20th, 2018]

Srivastava, A., Prasad, R., 2000, Triglycerides-based diesel fuels, Renewable and Sustainable Energy Reviews, Vol. 4, pp. 111-133

Wu, J., Shi, J., Fu, J., Leidl, J., Hou, Z., Lu, X., 2016, Catalytic Decarboxylation of Fatty Acids to Aviation Fuels over Nickel Supported on Activated Carbon, Scientific Reports, 6:27820, pp 1-8

APPENDICES

APPENDIX I GC A-% and mol data

APPENDIX 1 GC A-% and mol data

Table I Catalyst size experiments' GC results and calculated moles of C16:0 in each sample.

0,15-0,35 mm				
Sample	1	2	3	4
Time, h from 1st sample	0,00	1,13	2,52	3,08
C16:0, GC-A%	77,38	64,89	17,91	0,89
C16:0 total reacted, mol	0,09	0,16	0,33	0,38
1-1,7 mm				
Sample	1	2	3	4
Time, h from 1st sample	0,00	1,05	2,22	-
C16:0, GC-A%	92,64	84,92	72,95	-
C16:0 total reacted, mol	0,03	0,08	0,14	-
Half size				
Sample	1	2	3	4
Time, h from 1st sample	0,00	1,15	2,52	-
C16:0, GC-A%	95,08	87,19	74,81	-
C16:0 total reacted, mol	0,02	0,07	0,14	-
Full size				
Sample	1	2	3	4
Time, h from 1st sample	0,00	1,08	2,37	3,97
C16:0, GC-A%	88,90	78,71	65,89	64,50
C16:0 total reacted, mol	0,03	0,06	0,12	0,18

Table II Mixing speed experiments' GC results and calculated moles of C16:0 in each sample.

540 rpm			
Sample	1	2	3
Time, h from 1st sample	0,00	0,88	1,82
C16:0, GC-A%	78,11	59,04	39,32
C16:0 total reacted, mol	0,09	0,18	0,26
100 rpm			
Sample	1	2	3
Time, h from 1st sample	0,00	0,90	1,73
C16:0, GC-A%	41,63	5,84	0,22
C16:0 total reacted, mol	0,00	0,24	0,37

Table III Experiments with variable feed/catalyst ratio for palmitic acid.

FC 15			
Sample	1	2	3
Time, h from 1st sample	0,00	0,93	1,85
C16:0, GC-A%	80,13	61,02	43,33
C16:0 total reacted, mol	0,08	0,17	0,25
FC 31 (Basket)			
Sample	1	2	3
Time, h from 1st sample	0,00	1,13	2,33
C16:0, GC-A%	92,87	88,74	82,03
C16:0 total reacted, mol	0,04	0,08	0,13

Table IV Temperature and pressure experiments GC data and calculated molar values (335 °C, 20 bar)

335 °C, 20 bar					
Sample	Packed	1	2	3	4
Time, h from 1st sample	-	0,000	0,633	1,351	1,839
C16:0, GC-A%	98,938	87,493	83,287	78,625	74,809
C16:0, mol	0,435	0,379	0,346	0,313	0,287
C16:0/C16:0 initial	1,000	0,871	0,796	0,719	0,660
C15-C15 -ketone, GC-A%	0,000	8,863	13,075	17,463	21,246
C15-C15 -ketone, mol	0,000	0,022	0,031	0,040	0,046

Table V Temperature and pressure experiments GC data and calculated molar values (345 °C, 17 bar)

345 °C, 17 bar					
Sample	Packed	1,000	2,000	3,000	4,000
Time, h from 1st sample	-	0,000	0,459	0,940	1,375
C16:0, GC-A%	98,938	87,692	83,063	77,534	73,695
C16:0, mol	0,435	0,380	0,342	0,307	0,280
C16:0/C16:0 initial	1,000	0,873	0,787	0,705	0,643
C15-C15 -ketone, GC-A%	0,000	8,540	13,527	18,654	22,306
C15-C15 -ketone, mol	0,000	0,021	0,032	0,042	0,048

Table VI Temperature and pressure experiments GC data and calculated molar values (355 °C, 20 bar)

355 °C, 20 bar					
Sample	Packed	1,000	2,000	3,000	4,000
Time, h from 1st sample	-	0,000	0,459	0,940	1,375
C16:0, GC-A%	98,938	71,604	64,793	58,888	51,073
C16:0, mol	0,435	0,304	0,260	0,225	0,187
C16:0/C16:0 initial	1,000	0,698	0,598	0,517	0,429
C15-C15 -ketone, GC-A%	0,000	23,769	30,030	34,891	42,399
C15-C15 -ketone, mol	0,000	0,057	0,069	0,076	0,088

Table VII Temperature and pressure experiments GC data and calculated molar values (335 °C, 10 bar)

335 °C, 10 bar					
Sample	Packed	1,000	2,000	3,000	4,000
Time, h from 1st sample	-	0,000	0,651	1,469	1,969
C16:0, GC-A%	98,938	76,846	72,917	67,407	62,708
C16:0, mol	0,435	0,328	0,300	0,269	0,242
C16:0/C16:0 initial	1,000	0,754	0,690	0,617	0,556
C15-C15 -ketone, GC-A%	0,000	18,801	22,653	27,930	32,462
C15-C15 -ketone, mol	0,000	0,046	0,053	0,063	0,071

Table VIII Temperature and pressure experiments GC data and calculated molar values (355 °C, 10 bar)

355 °C, 10 bar					
Sample	Packed	1,000	2,000	3,000	4,000
Time, h from 1st sample	-	0,000	0,286	0,571	0,869
C16:0, GC-A%	98,938	79,718	75,167	70,200	62,702
C16:0, mol	0,436	0,342	0,310	0,279	0,240
C16:0/C16:0 initial	1,000	0,785	0,711	0,641	0,550
C15-C15 -ketone, GC-A%	0,000	15,938	20,447	25,076	31,540
C15-C15 -ketone, mol	0,000	0,039	0,048	0,057	0,069